Instrument Science Report WFC3 2012-08

Considerations for using Spatial Scans with WFC3

P. McCullough & J. MacKenty
May 02, 2012

ABSTRACT

We discuss considerations for preparing observations using spatial scans with WFC3 for two categories of intended reader: 1) the general observer preparing an observation, and 2) a contact scientist reviewing a phase 2 proposal. Coincidentally and conveniently, the IR spectroscopic Exposure Time Calculator's "brightest pixel" value in electrons accurately predicts (within 5%) the peak value of a spatially-scanned IR spectrum in digital numbers per pixel (DN/pixel).

Introduction

Spatial scans were re-introduced to the Hubble Space Telescope (HST) in April 2011 under an engineering test program 12325 (Figure 1). In preparing for that test and in subsequent development, now spanning approximately a dozen HST programs (Table 1), we have gained experience in using spatial scans and herein aim to record that experience for the benefit of others. Many of the observations in Table 1 would have failed if not for a contact scientist or other reviewer recognizing an error prior to the observations.

This document is organized as a checklist that an observer may use to prepare an HST phase 2 proposal, or a contact scientist may use to review such a proposal. Throughout this document, we reference HST program numbers and visits. These can be inspected on the STScI website, or more thoroughly with the Astronomer's Proposal Tools, APT.

Each of the recommendations herein should be considered carefully because detailed circumstances may change, and best practices will continue to improve.

Is spatial scanning indicated?

The first question to answer: "is spatial scanning indicated?" Potential benefits are 1) reducing overhead for time-series of short exposures due to detector operations required before and after each exposure, 2) avoiding saturation for very bright stars, 3) potentially improved photometry or astrometry due to collecting more photons per HST orbit. Potential disadvantages are 1) STScI pipelines do not work on spatially-scanned IR data so the observer will need to reduce data themselves, 2) world-coordinate-system headers will be confused, 3) astronomical sources will overlap more often than with staring-mode observations, especially for spectra, and 4) within an HST visit, the scan's start time (and hence location on the detector) can occasionally be late, compared to nominal, by 1, 2, or 3 seconds, due to synchronization of flight computers.

Spatial scans can be used with either the UVIS detector or the IR detector, and with direct imaging or (slitless) spectroscopy. In the following report, spatially scanned spectra are emphasized (Figure 1). Throughout, for sake of simplicity, we assume that for IR spectroscopy, the observer desires the $+1^{st}$ order spectrum.[1] In some special cases (e.g. observations of Vega in Visit 1 of HST program 12336), a different spectral order is used to reduce the grism's efficiency to avoid saturation of very bright stars: choosing a different order than the $+1^{st}$ order will affect nearly all the choices listed below.

IR MULTIACCUM Sample Sequence?

WFC3 IR observations use MULTIACCUM sample sequences, and while they can be useful for spatial scans, they are not as fundamental as they are for staring-mode observations. Typically in the analysis of spatially scanned observations, one forms an image in which each pixel is the difference between the last readout and the first readout, essentially a correlated double sample, or CDS. Whether the "first" readout is the 0th readout or the 1st readout, or even a later readout may depend on the particulars of a specific observation, and somewhat arbitrary choices of the analyst. For instance, if the spatial scan synchronization is imperfect, and the speed of the scan is still accelerating at the moment of the 0th readout, the analyst may choose to form the CDS using the 1st readout instead. The analyst may also wish to form all adjacent differences, 1st-0th, 2nd-1st, 3rd-2nd, etc, and analyze them independently; this may be useful to identify and subtract cosmic rays. Similarly, scanned stellar spectra of two stars that overlap (superpose) in a "last minus first" CDS pair could be separated temporally into their individual stellar

[1] Observers contemplating using the UVIS grism will find its spectral traces are curved with much order overlap, both of which will (significantly) reduce the likelihood of spatial scanning being effective.

spectra by forming appropriate intermediate-value CDS pairs and then subtracting one pair from the other to isolate one star's spectrum.[2]

Although analysis techniques are beyond the scope of this report, for spatially-scanned observations with WFC3 IR, the FITS headers of the *spt.fits* files contain keywords related to spatial scans in a section labeled "PROPOSAL INFO: Spatial Scan Info"; two examples of note are SCAN_RAT and SCAN_LEN, the scan rate in arcsec s^{-1} and the scan length in arcsec, respectively. We recommend the analyst begin with *raw.fits* images or the *ima.fits* images. Ironically, the *flt.fits* and *drz.fits* images of spatially scanned observations are essentially useless for IR data, except perhaps as "modern art," because the STScI pipeline attempts to fit a slope "up the ramp" of the MULTIACCUM, under the assumption (generally valid for staring-mode imaging) that the rate of charge accumulation in each pixel is spatially varying but time invariant. For a spatial scan, however, the rate of charge accumulation nearly everywhere on the detector is nearly zero, nearly all the time, except for a brief moment when the rate rises upward quickly and then rapidly fades, as a star's light scans over a given pixel. Also, whereas with staring-mode observations one can analyze earlier samples in the MULTIACCUM sequence to avoid saturation, with spatial scans, that post-observation analysis technique will not work – limiting the analysis to earlier readouts only truncates a star trail's length not its DN/pixel.

Because one of the potential benefits of spatial scans is reducing overhead in time series, one also generally desires to not interrupt the time series in order to dump a buffer. Observers may select sample sequences with small values of NSAMP, and small subarrays, so that no buffer dumps are required during the entire HST visibility period; for example, program 11622 observed the star GJ 436 without interruption using subarray GRISM256, sample sequence SPARS10, and NSAMP=2 in APT, meaning three samples are recorded per exposure. We estimate that the buffer can hold as many as 170 such exposures.[3]

Scan Rate?

The scan rate can be any real number between 0.0 and 7.84 arcseconds s^{-1}. Rates between 0.0 and 1 arcseconds s^{-1} have been demonstrated under FGS control, and higher rates can be accommodated without FGS control, hereafter referred to as "gyro control."[4]

---

[2] Given detector nonlinearity and charge persistence, this technique may require more complicated analysis than simple superposition. We recommend not to overlap spectra, if practical.

[3] Estimated as follows: 170 = 2*16*1024*1024 / (3*256*256), i.e. the numerator is the buffer size, equivalent to two 16-sample full-frame IR images, and the denominator is the three samples per exposure times the subarray's size.

[4] HST uses gyros at all times to maintain spacecraft pointing, regardless of whether the FGS are used also. Here, the phrase "gyro control" means "without FGS control."

(A change expected after HST Cycle 19 will allow FGS control up to 5 arcseconds s^{-1}.) A rate of 7.5 arcseconds s^{-1} has been demonstrated under gyro control in program 12713.

The observer needs to calculate a scan rate to achieve a desired exposure level on the detector. The online exposure time calculators (ETCs) do not currently include spatial scans *per se*, but one can estimate by scaling from the ETC's predictions for "brightest pixel counts."

Based upon Visit 2 of program 12325, in which we scanned the M4.5 V star GJ 1214, H=9.09 mag, at 0.1 arcsec/s with the G141 grism, and the peak was 12670 DN/pixel, we can predict the peak DN/pixel in G141 for any rate and H mag:

$$\text{Flux (DN/pixel)} = (5.5 / R) * 10^{-0.4(H-15)} ,$$

where R is the scan rate in arcsec s^{-1} and H is the Bessel H band magnitude.

The WFC3 IHB, section 7.9.1 states the full well of the IR detector is 33,000 DN, so if we wish to avoid that with some margin, say keep the peak flux below 25,000 DN, then we should use a scan rate

$$R \text{ (arcsec } s^{-1} \text{)} = 10^{-0.4*(H-5.9)},$$

which implies that for stars with 4.15 > H > 3.7 mag, WFC3 G141 spectra can be obtained with less than 25,000 DN/pixel only under gyro control, i.e. R = 5.0 to 7.8 arcsec s^{-1}. For FGS control, limited to R < 5 arcsec s^{-1}, the same detector limit (25,000 DN/pixel) requires H > 4.15 mag for G141 spectra.

For three examples, we compare in Table 2 actual observations to predictions by the WFC3 IR spectroscopic ETC of the brightest pixel and recommend an appropriate scale factor for observers to estimate the peak count rates for their own spatially-scanned observations.

Table 2: Scale factor to be applied to ETC Predictions

Grism	Star	Type	Mag	Exposure (sec)	Peak(Obs) (DN/pix)	Peak(ETC) (e/pix)	Ratio (DN/e)	Program Number
G141	GJ1214*	M4V	H=9.09	1.210	12670	10855	1.17	12325
G141	GJ1214*	M5V	H=9.09	1.210	12670	12540	1.01	12325
G141	XO-1	G1V	H=9.60	2.420	18000	18200	0.99	12181
G141	HD189733	K1V	K=5.54	0.122	32000**	32900	0.97	12181

*Because GJ214 is specified as M4.5 V in the literature, and the ETC only allows M4 V or M5 V, we have listed GJ 1214 twice, with values appropriate for each spectral type.
**This exceeds the maximum value (25,000 DN) recommended in this report, but it was the best that could be done at the time. It used the maximum scan rate under FGS control available at the time, 1 arcsec s^{-1}.

In Table 2 above, the exposure time listed is derived simply by dividing the size of an IR pixel (0.121 arcsec in the Y direction) by the scan rate in arcsec s^{-1}, the peak (observed) pixel is estimated from *raw.fits* images of spatially scanned spectra, and the peak (ETC) is the value reported for the "brightest pixel" by the WFC3 ETC for the characteristics given in Table 2 and tacitly for staring-mode imagery. For spatially scanned spectra, the counts in a pixel accumulate over the full extent of the line spread function (LSF) perpendicular to dispersion: temporally, the pixel "sees" the leading wings of the LSF, then its core, then the trailing wings of the LSF. With that in mind, we expect analytically that the ratio listed in column 8, Peak(Obs)/Peak(ETC) to equal 0.96 DN/electron, which we derive from the ratio of the column-integrated flux to the peak pixel, 2.27 for G141 from the ETC[5], divided by the IR detector gain (2.38 e/DN).[6]

Given the uncertainties associated with the detector gain, we consider the agreement (within ~4%) between the values in Table 2 and the analytic expectation to be adequate for us to recommend using the ETC for the purposes of estimating a scan rate to achieve a specific exposure level. **Coincidentally and conveniently, the IR spectroscopic ETC's "brightest pixel" value in electrons accurately predicts the peak value of a spatially-scanned spectrum in DN/pixel.** As noted, that simple rule of thumb has been verified for the G141 grism. For the G102 grism we lack appropriate observations, spatially-scanned G102 spectra at moderate exposures, to make a direct comparison to the ETC. However, the ETC predicts for the G102 grism that the ratio of column-integrated flux to the peak pixel is 2.17, so we expect the scale factor for G102 is 0.96 DN/electron, i.e. 4% less than G141's value of 1.0 DN/electron.

An alternative method of estimating the scan's intensity is as follows.[7] In the IR spectroscopic ETC, set the number of rows to the maximum (1x9 pixels, to collect nearly all the light), then use the total number of electrons s^{-1} predicted by the ETC at the brightest wavelength, multiply by the total time for the scan, and divide by the length of the scan in pixels. The result will be the peak intensity, in electrons per pixel.

On the topic of choosing a scan rate to avoid saturation, we note that a commonly adopted definition of saturation for the WFC3 IR detector is the level at which a pixel's measured nonlinearity correction exceeds 5% (Hilbert 2009). Figure 11 of Hilbert (2009) illustrates the distribution of saturation level (by the 5% definition) for all pixels, and he notes that 2.6% of the light-sensitive pixels are "saturated" at signal levels below 28,000 DN. However, the IR detector's response is nonlinear throughout its range, and depending on the scientific requirements of any particular observation, exposing the detector significantly less than saturation may be indicated. We note that the observations of GJ 1214 and XO-1 listed in Table 2, with peak counts of 12670 and 18000 DN/pixel

---

[5] We divide the sum of a 1x9 pixel rectangle by the value for the brightest pixel, and then divide that by the encircled energy fraction of 0.92; all three values are given by the ETC.
[6] The mean of the range 2.28 to 2.47 e/DN (WFC3 Instrument Handbook, Table 5.1).
[7] Thanks to Drake Deming for this suggestion.

respectively, have enabled precision exoplanet spectra with the G141 grism (McCullough 2011a, 2011b, and 2012; Deming 2012).

FGS or Gyro control?

In some cases, the decision whether to observe under FGS control or gyro control is dictated by the scan rate (see previous section). There are some other considerations too.

FGS feedback introduces jitter into the positioning of a star throughout the scan (Figure 2). The FGS jitter during spatial scans is comparable to that of staring-mode observations (~0.0035 arcsecond r.m.s. in each of two orthogonal axes, Bradley 2011), however its effects on spatial scans are more noticeable: jitter parallel to the scan direction creates apparent brightness variations along the trail ("flicker" or "scintillation"), and jitter perpendicular to the scan direction creates imperfectly straight and narrow trails (i.e. the trail "wanders").

Under gyro control, trails are smoother because they lack the FGS feedback and its effects just described. On the other hand, as with any HST observation under only gyro control, unpredictable drifts are expected at a nominal rate of 0.001 arcsecond s^{-1}, so the scan rate potentially is inaccurate by that amount. Also, if repeatedly positioning a target, either a direct image's PSF or a spectrum, on the same pixels of a sensor throughout an HST orbit is important, e.g. as in a time-series of exoplanet transit spectra, FGS control is indicated.

Scan Orientation?

The scan orient (orientation angle) is defined such that 90 degrees is parallel to the Y-axis of the POS TARG coordinate system (see Figure 6.1 of the WFC3 Instrument Handbook). The scan orient should be 90 degrees in order for spectra to be extended along columns, i.e. very nearly perpendicular to dispersion, and also for star trails to be parallel to columns on either of the detectors (i.e. for scans "in the Y direction on the detector").

In order for star trails to be parallel to rows (i.e. for scans "in the X direction on the detector"), the scan orient should be 3.7702 degrees for the UVIS detector, and 0.1738 degrees for the IR detector.[8] Those values are different and non-zero due to geometric distortion in the instrument optics (Figure 3). They will only be useful for imaging, not spectroscopy, because spectra are dispersed in the X direction.

In some cases one may intentionally trail stars at an angle to rows or columns, in order to sample pixel phase. An example is Program 12679, which set the scan orient =

[8] Merle Reinhart analytically calculated these angles for the center of each detector; they were successfully demonstrated as Visit 1B (WFC3 UVIS) and 2A (WFC3 IR) of Program 12713.

90.05 degrees: the extra 0.05 degrees trailed the stars ~3.2 pixels in X for every 3700 pixels in Y.

Visit Orientation?

One should take care that the slitless spectra of field stars does not contaminate that of the target. While that is also true for staring-mode observations, it is particularly important for spatially scanned spectra because the area of each spectrum on the detector can be very large.

An example in which visit orientation is especially important is Visit 26 of Program 12473, in which Sing et al. use spatial scanning to observe the double star HAT-P-1 with WFC3's G141 grism.[9] They want to keep the two stars' scanned spectra separate on the detector, as much as practical. (A visual double star with overlapping scanned spectra appears in Figure 1, along with the comparable staring-mode spectra that do not overlap because the spectra are not as "tall" on the detector.) The star with a transiting exoplanet, HAT-P-1, has a companion, 0.5 mag brighter, with a separation of 11.2 arcseconds at a position angle of 253 degrees. For convenience, they define their target to be the midpoint on the sky between the two components of the double star, and they aim to observe both stars simultaneously on the detector. For maximum separation of the two spectra, they want the two stars' zeroth-order light to have the same X position on the detector, or equivalently, the vector connecting the two stars to be parallel to the Y axis of the detector. Section 8.2 of the WFC3 IHB specifies that "orient ~135 degrees aligns the Y axis of the detector with North." Hence, the ideal orient = 135+253 = 388 = 28 degrees (or 208 degrees) will align (or anti-align) the Y axis of the detector with the vector pointing from the bright star to the faint star. Sing et al. prescribe for Visit 26 an orient range of 168 to 248 degrees, i.e. 208±40 degrees, because 208 is one of the two ideal angles[10], and 40 degrees is slightly less than the maximum deviation from the ideal visit orient that still keeps the spectra from overlapping, because each scanned spectrum will be 7.0 arcseconds tall (46.7 second exposure at 0.15 arcsec s^{-1}) and the two stars are separated by 11.2 arcseconds. In order to have some margin to cleanly separate the two spectra, the half-angle tolerance (40 degrees in this case) should be smaller than $\cos^{-1}$ (EXPTIME * SCAN RATE / SEPARATION) = $\cos^{-1}$ (46.7 s * 0.15 arcsec s^{-1} / 11.2 arcsec) = 51 degrees. The observer can assess how much margin will suffice, a judgment that must balance a wider separation against a narrower window on the calendar to schedule the observation.

---

[9] Sing et al. refer to HAT-P-1 as HAT-1.

[10] Sing et al. could have added a second visit orient range, 28 degrees +- 40 degrees, specified in APT as 348 to 359.99 degrees and 0 to 68 degrees.

Scan direction?

For a spatial scan, the intent is that the target moves from point A to point B at a constant angular rate on the sky.[11] Scans can be either "forward" or "reverse." The default is "forward." Whether a scan is "forward" or "reverse," point A is intended to be equal to the location that a staring-mode image would have been. Point B is derived from the scan rate and orientation, and also does not depend on whether the scan is "forward" or "reverse." For forward scans, the target moves from A to B. For reverse scans, the target moves from B to A. The intent is for the target to cross point A (for a forward scan, or point B for a reverse scan) at the moment 1) of shutter opening (UVIS) or 2) the final reset before an IR exposure commences.

For repeated observations, such as a time series of stellar spectrophotometry, the observer needs to select between two natural choices: 1) repeated "forward" scans, or 2) repeated pairs of "forward" then "reverse" scans. There is no established guidance for this choice as of the time of publication of this report. Choice 1 may be advantageous if the observer requires all the images to be as similar as possible, because we anticipate small systematic offsets in positioning between forward and reverse scans. However, choice 1 has two potential disadvantages related to its "rewinding" the telescope to prepare for the next forward scan: 1) larger overhead, because the time spent "rewinding" isn't used for gathering data, and 2) during "rewind" the scan rate is not at a constant rate like the actual scans, and the detector is still exposed to star light and yet that star light is not recorded by the detector. The second potential disadvantage is subtle: one doesn't know what star light may have fallen on which pixels of the detector, possibly leaving after images due to charge persistence. The potential advantages of pairs of "forward" and "reverse" scans are simply the complement of the disadvantages of the alternative: 1) less overhead, and 2) the "rewind" is observed and recorded. At the present time, an undeniable advantage of repeated "forward" scans is convenience of defining many of them in the Astronomer's Proposal Tools (APT): simply set "number of iterations" for your exposure to N > 1 and it will repeat the forward scan N times. On the other hand, repeated pairs of "forward" and "reverse" scans must be tediously defined as single exposures in a (potentially very long) APT file.

Discussion of the effects of charge persistence on IR data quality is beyond the scope of this report. We note simply that charge persistence for the IR detector is observed for spatially scanned data much as it is for staring-mode. For guidance, see http://www.stsci.edu/hst/wfc3/ins_performance/persistence/ and individual Instrument Science Reports at http://www.stsci.edu/hst/wfc3/documents/ISRs/ . Given the very

[11] The intent is that HST will scan a great circle on the sky at a constant angular rate, centered on the target, at the prescribed orientation angle in sky coordinates. No corrections are made to the scan rate for geometric distortion in HST or the WFC3 instrument.

different spatial and temporal exposure to light of spatially scanned images compared to staring-mode images, we would not be surprised if differences appear in the behavior of the charge persistence in each case.

Up-stream/Down-stream effect?

The so-called "upstream/downstream" effect applies only to the IR detector.[12] Because of the upstream/downstream effect, described below, observers are advised to keep star trails or trailed spectra from crossing the Y=512 boundary if practical to do so and if the most precise photometry or spectrophotometry is required.

For the IR detector, stars moving toward the middle row of the detector are moving "downstream" with respect to the readout direction (i.e. for every raster-scanned readout pattern, whether for full-frame or subarrays, pixels nearer the top (Y=1024) and bottom (Y=1) of the detector are read first, and pixels at the middle of the detector are read last). For scans not in the X direction[13], the total flux of a star trail (of trailed spectrum) integrated over its entire length on an IR image will depend on the whether the scan is "upstream" or "downstream" of the read out of the quadrants of the IR detector. For example, if the scan is downstream, (again, the star is moving in the same direction as the readout), then the total integration time from first read to last read will be slightly longer than if the star had been moving "upstream." (Obviously, the nominal exposure time recorded in the FITS header is only approximate for scanned targets.) The magnitude of the upstream/downstream effect depends on the ratio of the angular scan rate projected along the Y axis to the readout rate in rows per second, and the latter depends on the specific subarray (Petro & Wheeler 2006). As an example, in program 12325's observations with a 512x512 subarray, the re-normalization factor to account for the upstream/downstream effect is 1±0.853027/(512/2), or 1±0.0033.

POS TARG?

The observer should use POS TARGs in X and Y, each in arcseconds, to place their target at the desired location on the detector; this is especially important for subarrays. <u>We assume the observer has entered correctly their target's position and proper motion</u>.

---

[12] The mechanical shutter for the UVIS detector is approximately 100 times faster (in apparent velocity in pixels per second) than the IR detector's read out rate (in rows per second). Consequently, the upstream/downstream effect is negligible for the UVIS detector.

[13] There is also an upstream/downstream effect for scans in the X direction, although it is much smaller than the effect we are discussing, because the detector readout rate in columns per second (for any given row) is much higher than the readout rate in rows per second. How much higher? Approximately equal to the number of pixels in each row of each quadrant of each subarray (minimum, 32; maximum, 512).

As an example, we examine Visit 7 of Program 12181, a spatially scanned G141 spectrum of the exoplanet host star XO-1 during a transit of its planet XO-1b. The IR sample sequence SPARS10-8 produces a 50.3-s exposure, and at a scan rate of 0.05 arcsec s^{-1}, that's a spectrum height of 2.515 arcsec, or 20.8 pixels at a scale of 0.121 arcsec/pixel in Y. The observer specified POS TARG in X = 0.0 arcsec, because the selected aperture, GRISM128, automatically intends to center the G141 spectrum in X (Figure 4). Actually, for GRISM128, the 128-pixel subarray isn't quite wide enough to capture the G141 first-order spectrum in its entirety so the subarray crops the spectrum's long wavelength end (at ~1.6 microns). The aperture definition[14] (Y reference position = 522 for aperture GRISM128) intends to center the aperture 10 pixels higher in Y than the center row of the 1024x1204 IR detector. Recognizing that, the observer specified POS TARG in Y = -1.3 arcsec, in order to shift the scan's starting point "A" approximately at the center of the array, at Y = 522 – 1.3/0.121 = 511.3, and in that case, the scan's end point "B" to Y = 511.3 + 20.8 = 532.1. (Aiming point "A" near the detector's center may be wise if one is concerned about the target missing the subarray entirely. Errors in target position (and proper motion), guide stars' positions, and timing synchronization, all can cause pointing uncertainty for a spatial scan. Stellar positional uncertainties are typically less than 1 arcsecond, so the unpredictable 0, 1, 2, or 3-second delay in the start of the scan with the start of the exposure can be the dominant positional error for rapid scans. Engineers expect any delay to be fixed within a visit. Limited experience suggests that the most common delay is 0 seconds, i.e. correct synchronization.) As we mentioned earlier, we recommend that the target spectrum not cross the Y=512 boundary between amplifiers. In retrospect, the Y POS TARG could have been, say, 0 arcsec, and the spectrum would have covered rows from Y=522 to Y=542.8, and arguably that would have been a slightly better choice, because the GRISM128's upper two amplifiers readout rows Y=513 to Y=576, and thus the position of the spectrum would have been well centered in the bottom half of the top two quadrants, allowing the top half of those same quadrants for empirical "sky" subtraction.

As second example, we examine Visit 1 of Program 11622, a spatially scanned G141 spectrum of the exoplanet host star GJ-436 during a transit of its planet GJ-436b. The IR sample sequence SPARS10-2 produces a 7.6-s exposure, and at a scan rate of 0.99 arcsec s^{-1}, that's a spectrum height of 7.6 arcsec, or 62.8 pixels at a scale of 0.121 arcsec/pixel in Y. The observer specified POS TARG in X = 0.0 arcsec, for the same reason as for the first example, although in this case the aperture is GRISM256. The aperture definition for aperture GRISM256 intends to center the aperture at Y =532, i.e. 20 pixels higher in Y than the center row of the 1024x1204 IR detector. For an associated direct image using aperture IRSUB256, which has a reference position Y = 522, the observer selected a Y

[14] http://www.stsci.edu/hst/observatory/apertures/wfc3.html

POS TARG = 5.3 arcsec so that the star would land at Y = 522 + 5.3/0.121 = 565.8, which is ~10 pixels below the middle of the top two quadrants of GRISM256. The observer also chose to approximately center the 7.6-arcsec-tall, spatially-scanned G141 spectrum at the same Y position as the direct image with a Y POS TARG = +1.5 arcsec, because +1.5 arcsec = +5.3 arcsec – (7.6 s)*(0.99 arcsec s^{-1})/2.

Boustrophedonic Scans

Boustrophedonic (from the Greek, literally, "as an ox turns in plowing") scans, are possible too, for calibration purposes.[15] In boustrophedonic scans, the user specifies a set of constant-speed scan lines separated by a specified angular distance, like rows in a farmer's field. An example is HST program 12713, in which bright double stars were trailed repeatedly all the way across the detectors, specifically for validation of the low-spatial-frequency flat fields (Figure 3).

Conclusions

This report is a guide for observers and STScI contact scientists in best practices for spatial scans. We reference many examples from many different scientific programs and calibrations programs. The most commonly cited example is that of an observation of a spatially-scanned, IR spectrum of an exoplanet host star. Such an observation is akin to the lighting of a proverbial set of Christmas tree lamps in series: if a single bulb burns out, the entire set will not light. Likewise, if a single mistake occurs in preparing one of these spatially-scanned observations, the entire program may be ruined.

The authors wish to thank the many persons that contributed to re-enabling spatial scans on HST: the TRANS, Spike, and APT teams at STScI; engineers at GSFC and subcontractors of GSFC; scientists at STScI, and especially the HST observers that have helped us pioneer this new capability. An incomplete list of contributors include Art Bradley, Stefano Casertano, George Chapman, Drake Deming, Susana Deustua, Mark Giuliano, Josh Goldberg, Bill Januszewski, John Lecourt, Larry Petro, Merle Reinhart, Adam Riess, Christine Ritchie, and Alan Welty. We also thank Bryan Hilbert, Nor Pirzkal, and Drake Deming, whose reviews improved this report.

[15] The nominal single-line scan actually is implemented as a degenerate case of a boustrophedonic scan.

References

Bradley, A. 2011, Spacecraft System Engineering Services, private communication of unpublished report "FGS Vehicle Scan (#52 Command) On-Orbit Test of 2011:083"

Deming, D. et al. 2012, "Infrared Spectroscopy of the Transiting Exoplanets HD189733b & XO-1 using HST/WFC3 in Spatial Scan Mode," oral presentation at the conference, American Astronomical Society, Jan 9-12, 2012, Austin TX USA

McCullough, P. R. & MacKenty, J. W. 2011a, "Spatial Scanning with HST for Exoplanet Transit Spectroscopy and other High Dynamic Range Observations," poster presentation at the conference, Exploring Strange New Worlds, May 1-6, 2011, Flagstaff AZ USA

McCullough, P. R., Berta, Z. K., Howard, A. W., & MacKenty, J. W. 2011b, "Spectroscopy of sub-Neptune-sized Planets GJ1214b and HD97658b with HST WFC3," poster presentation at the conference, First Kepler Science Conference, Dec 5-9, 2011, NASA Ames, CA USA

McCullough, P. R., Berta, Z. K., Howard, A. W., MacKenty, J. W. & the WFC3 Team 2012, "WFC3: Spatially-scanned Spectra of Exoplanet Transits (and more)," poster presentation at the conference, American Astronomical Society, Jan 9-12, 2012, Austin TX USA

Petro, L. 2010, "IR Grism Subarray Design and Use," (Internal) Technical Instrument Report, WFC TIR 2010-03

Petro, L. & Wheeler, T. 2006, New IR Detector Sample Times, WFC3 ISR 2006-06

Table 1: HST Programs using Spatial Scans*

Program, Title, Investigators, Targets

11622 A Search for Water and Methane on a Neptune-Mass Transiting Planet, Knutson, H. et al., GJ 436

12181 The Atmospheric Structure of Giant Hot Exoplanets, Deming, L. D. et al., HD 189733, XO-1, and HD 209458

12325 Photometry with Spatial Scans, MacKenty, J. W., & McCullough, P. R., GJ1214

12336 Scan Enabled Photometry, MacKenty, J. W., McCullough, P. R., & Deustua, S., Vega and other calibration stars

12449 Atmospheric Composition of the ExoNeptune HAT-P-11, Deming, L. D., et al., HAT-P-11

12473 An Optical Transmission Spectral Survey of hot-Jupiter Exoplanetary Atmospheres, Sing, D. K. et al., WASP-31, HAT-P-1

12495 Near-IR Spectroscopy of the Hottest Known Exoplanet, WASP-33b, Deming, L. D. et al., WASP-33

12679 Luminosity-Distance Standards from Gaia and HST, Riess, A., et al., Milky Way Cepheids

12685 Enabling Dark Energy Science for JWST and Beyond, Hines, D. C. et al., Calibration stars

12699 WFC3 Photometric Calibration & Calibration Flux Ladder, Deustua, S. E. et al., Calibration stars

12713 Spatial Scanned L-flat Validation Pathfinder, McCullough & MacKenty, nearly identical double stars

* The list does not include the very few HST programs that used spatial scans in the 20th century.

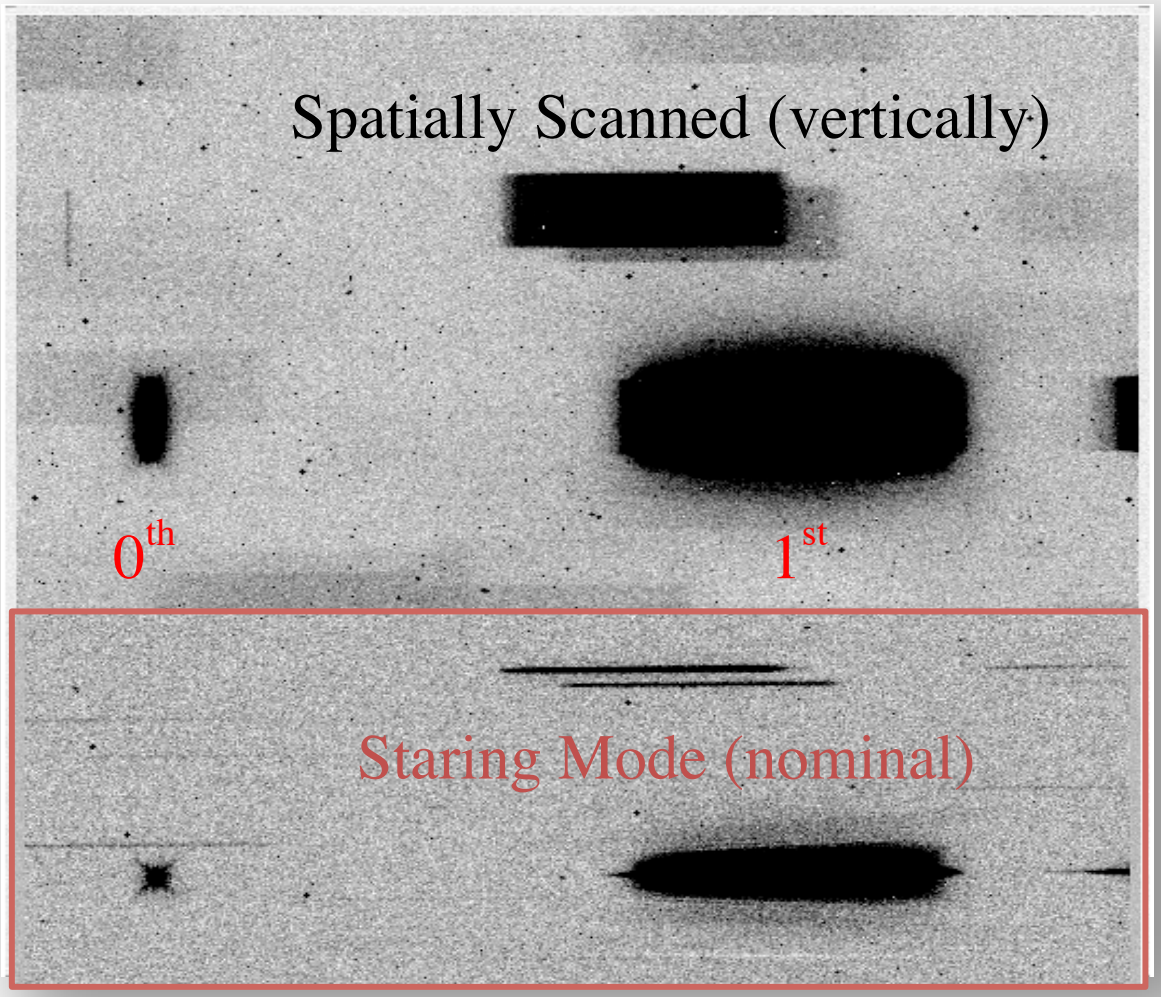

Figure 1: The spatially-scanned spectrum of the star GJ1214, from program 12325 (MacKenty, P. I.), labeled with its 0th and +1st order light, and compared to a nominal staring-mode slitless spectrum of the same field (red outlined inset). The images are 512 columns wide, of the detector's 1024. The scan was 40 pixels high (4.8 arcsec).

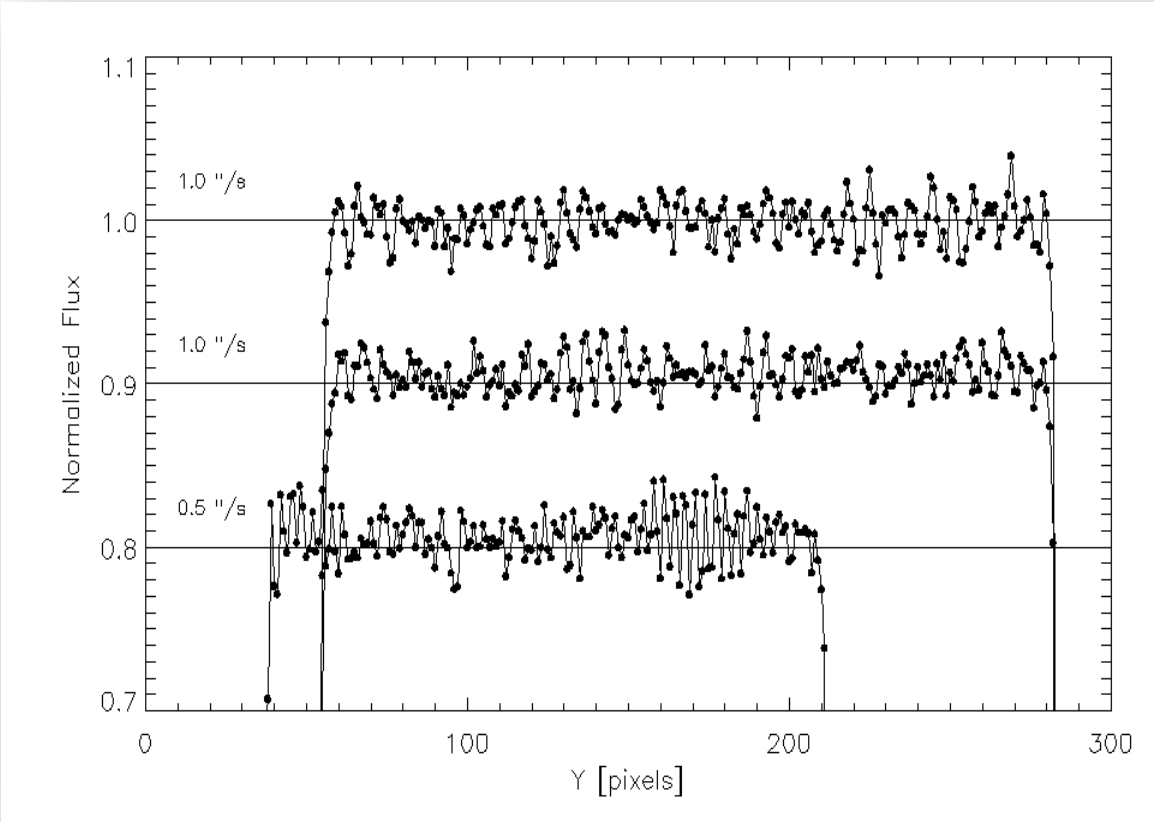

Figure 2: Photometric "flicker" appears in scans under FGS control. In program 12325, we trailed the star P330E across the WFC3 IR detector repeatedly, with rates of 1, 1, and 0.5 arcsec s^{-1} respectively. Photometry integrated transverse to each of the three trails, show intermittent oscillations with ~3% amplitude at ~1.3 Hz, due to image motion or "jitter" during the scans. The 2nd and 3rd trails have been offset vertically by 0.1 and 0.2 for clarity.

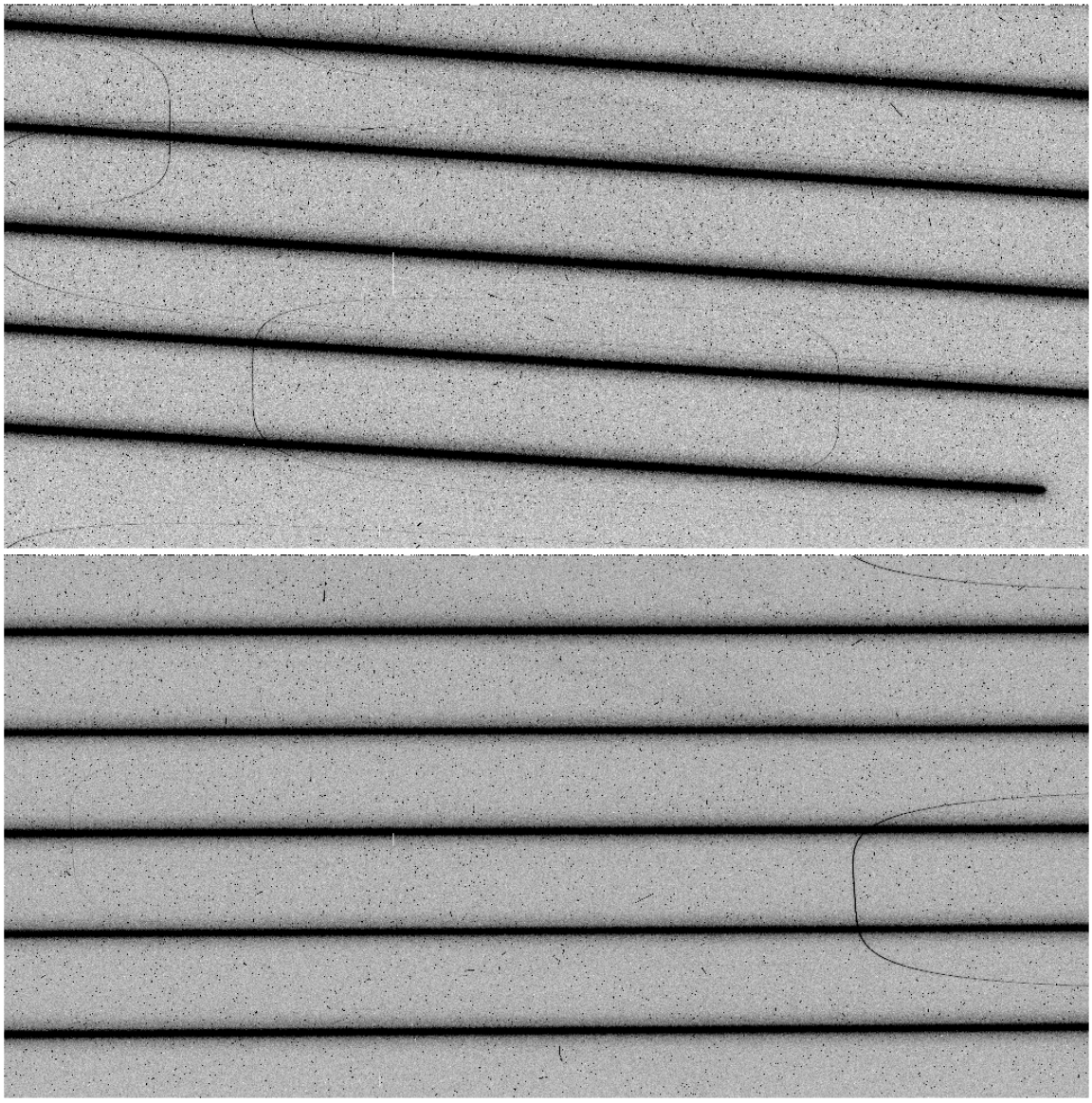

Figure 3: (Top) Image of a double star boustrophedonically scanned at scan orient 0 degrees results in trails tilted with respect to the UVIS CCD's rows. (Bottom) the "correct" non-zero scan orient aligns the scan precisely along rows (see text). The fainter U-shaped trails are from the turning points of nearby fainter stars. Images are from program 12713.

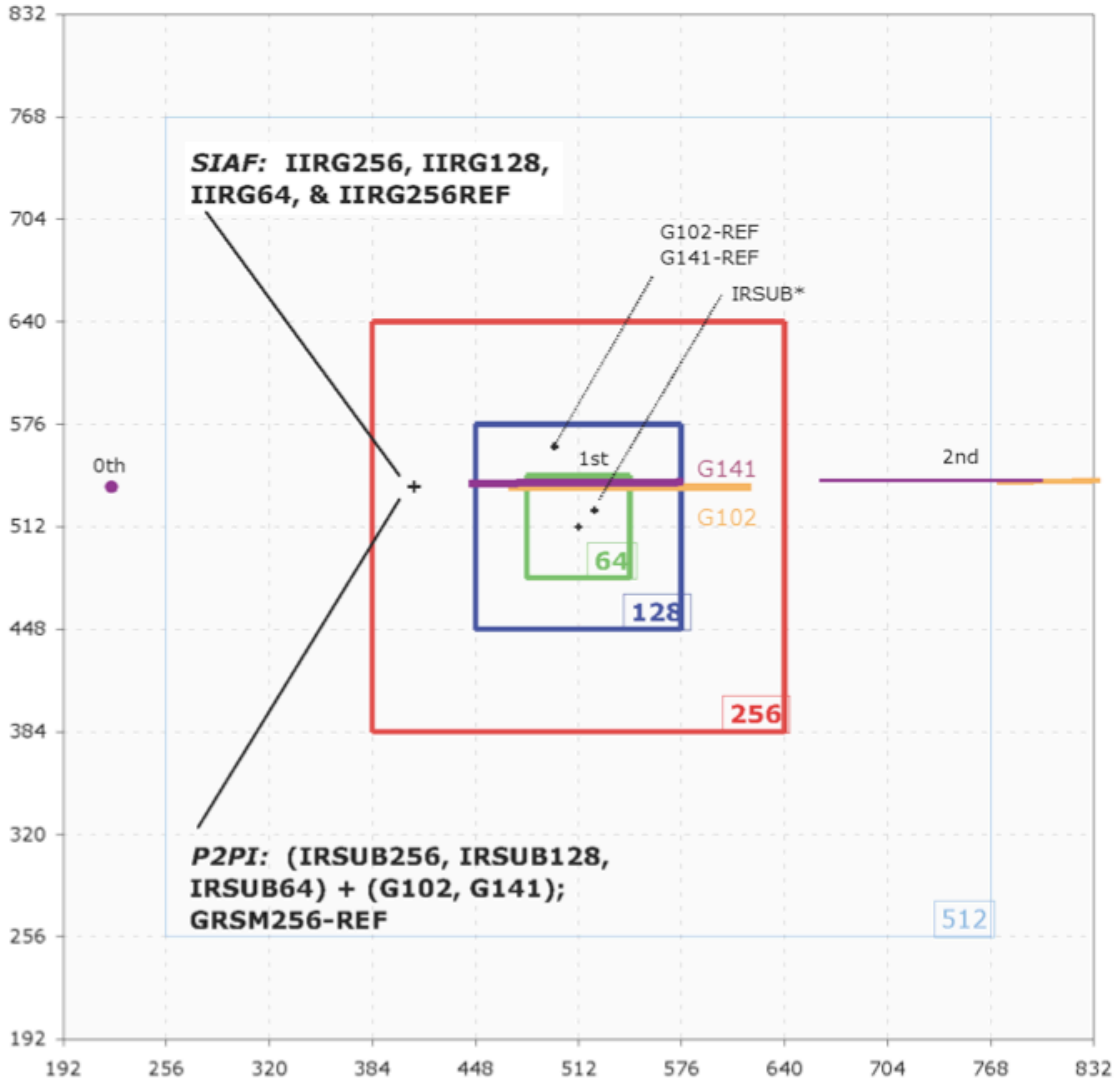

Figure 4: (Reprinted from Petro (2010), WFC3 Technical Instrument Report 2010-03 "IR Grism Subarray Design and Use," from data at http://www.stsci.edu/hst/observatory/apertures/wfc3.html). This illustrates the approximate locations (for zero POS TARG, staring-mode observations) of the G141 (purple) and G102 (yellow) spectra in relation to the GRISM64 (green), GRISM128 (blue), and GRISM256 (red) subarrays. As shown, the G141 first-order spectrum is approximately centered (in X) in the three subarrays. The G102 first-order spectrum is offset somewhat from center (in X). Spectra are located slightly above the quadrant boundary at Y=512. Because general observers do not have access to TIRs, the STScI contact scientist should discuss this diagram with the observer to ensure that the phase 2 proposal faithfully implements the observer's intentions.